Functional receptor molecules CD300lf and CD300ld within the CD300 family enable murine noroviruses to infect cells

Kei Haga[a,1], Akira Fujimoto[a,1], Reiko Takai-Todaka[a], Motohiro Miki[a,b], Yen Hai Doan[a], Kosuke Murakami[a], Masaru Yokoyama[c], Kazuyoshi Murata[d], Akira Nakanishi[e,2], and Kazuhiko Katayama[a,2]

[a]Department of Virology II, National Institute of Infectious Diseases, Tokyo 208-0011, Japan; [b]New Business Planning Division, Innovative Diagnostics Research Center, Denka Innovation Center, Denka Company Limited, Tokyo 194-8560, Japan; [c]Pathogen Genomics Center, National Institute of Infectious Diseases, Tokyo 208-0011, Japan; [d]National Institute for Physiological Sciences, Aichi 444-8585, Japan; and [e]Section of Gene Therapy, Department of Aging Intervention, National Center for Geriatrics and Gerontology, Aichi 474-8511, Japan

Norovirus is the leading cause of acute gastroenteritis worldwide. Since the discovery of human norovirus (HuNoV), an efficient and reproducible norovirus replication system has not been established in cultured cells. Although limited amounts of virus particles can be produced when the HuNoV genome is directly transfected into cells, the HuNoV cycle of infection has not been successfully reproduced in any currently available cell-culture system. Those results imply that the identification of a functional cell-surface receptor for norovirus might be the key to establishing a norovirus culture system. Using a genome-wide CRISPR/Cas9 guide RNA library, we identified murine CD300lf and CD300ld as functional receptors for murine norovirus (MNV). The treatment of susceptible cells with polyclonal antibody against CD300lf significantly reduced the production of viral progeny. Additionally, ectopic CD300lf expression in nonsusceptible cell lines derived from other animal species enabled MNV infection and progeny production, suggesting that CD300lf has potential for dictating MNV host tropism. Furthermore, CD300ld, which has an amino acid sequence in the N-terminal region of its extracellular domain that is highly homologous to that of CD300lf, also functions as a receptor for MNV. Our results indicate that direct interaction of MNV with two cell-surface molecules, CD300lf and CD300ld, dictates permissive noroviral infection.

norovirus proteinaceous receptors | CD300 molecules | CD300lf | CD300ld | murine norovirus

Human norovirus (HuNoV) belongs to the Caliciviridae family and is the leading cause of acute gastroenteritis worldwide. Since the discovery of HuNoV in 1972 (1), studies of the virus have been limited by the lack of an efficient cell-culture system for growing the virus. Recently, HuNoV was produced by using cultured human B cells (2); however, that system supports only a very limited amount of viral replication. Hence, neither the mechanism by which the norovirus establishes infection nor the receptor that allows permissive infection is currently known.

The closely related lagovirus, a member of the Caliciviridae, uses histo-blood group antigens (HBGAs) as receptors (3). HuNoV might also use HBGAs as initial binding factors (4–6), but other receptors are suspected to be involved. For example, although HuNoV GII.1 virus-like particles (VLPs) bind to intestinal biopsy samples (7, 8), in vitro VLP–HBGA binding assays show that GII.1 VLPs do not react with any type of HBGAs found in saliva (9). In addition, cells that overexpress HBGAs are not susceptible to infection by HuNoV. Although such cells support the replication, albeit only to a limited extent, of HuNoV RNA that was purified from the stool of infected patients and was transfected into cells (10), the viral progeny do not infect neighboring cells. Those results suggest the presence of unknown molecules in addition to HBGAs that are required for HuNoV infection into cells.

Murine norovirus (MNV) was discovered in 2002 as a lethal infectious agent in recombination-activating gene (RAG)/STAT1$^{-/-}$

mice that were deficient in STAT1 and RAG2 (11). MNV replicates within the murine macrophage cell line RAW264.7 cells. MNV strains MNV-1, WU11, and S99 bind macrophages ex vivo through a terminal sialic acid on the ganglioside GD1a, which has been suggested as a binding receptor (12). Another MNV strain, CR3, binds a different glycan, and the difference in glycan binding might contribute to tissue tropism in vivo (13). Those observations imply that the glycans on the cell surface are important for MNV binding to cells. It is not known, however, if a glycan also contributes to MNV internalization into cells.

Previously, we reported a plasmid-based reverse-genetic system of several HuNoVs, including the prototype Norwalk virus (NV68) strain (GI.P1_GI.1), U201 (GII.P3_GII.3), Saga-1 (GII.P4_GII.4), and TCH04-577 (GII.P21_GII.3) (14). Those constructs produce viral progeny, but the infectivity of the human strains could not be demonstrated because of the lack of a permissive cell system. In contrast, a construct of an MNV-S7 strain, which was initially isolated from mouse stool in Japan (15), produced infectious virions in several cell lines, including RAW264.7 cells and other non–mouse-derived cell lines such as HEK293T cells and COS7 cells. Taken together with the results of Guix et al. (10), our results showed that, if the norovirus genome is provided intracellularly, infectious particles can be produced even in cells that are not

Significance

Norovirus is the leading cause of acute gastroenteritis worldwide. Since the discovery of norovirus, a receptor for norovirus internalization into cells has not been identified. Murine norovirus (MNV) binding to cells that were originally not susceptible to the virus can be mediated by ectopically expressed CD300 molecule like family members f or d (CD300lf or CD300ld). The expression of CD300lf or CD300ld is sufficient to render cells permissive to infection by the virus. We conclude that CD300lf and CD300ld are essential for MNV infection and that each molecule can function independently as the viral receptor.

derived from the natural host. In other words, the norovirus host tropism is likely determined by an early event in the replication cycle, which could involve a receptor-dependent host process (10).

Here, we report our search for functional proteinaceous receptors for MNV infection. By using a clustered regularly interspaced short palindromic repeats/CRISPR-associated protein 9 (CRISPR/Cas9) system, we randomly knocked out genes in RAW264.7 cells. We collected the cells that escaped the cytopathic effect (CPE) of MNV and examined them for candidate genes by next-generation sequencing (NGS). We then tested the products of the candidate genes for their ability to function as MNV receptors.

Results

CD300lf Functions as a Receptor for MNV in RAW264.7 Cells. We sought to identify a functional receptor for MNV infection in RAW264.7 cells. MNV invokes a strong CPE in RAW264.7 cells, killing the majority of the cells by 48 h post infection (hpi). We performed a genome-wide genetic screening for the MNV receptor using a lentiviral CRISPR/Cas9 library (16). The library consists of 87,987 guide RNAs (gRNAs) targeting 19,150 mouse protein-coding genes, packaged into lentiviral vectors. We transduced the library into RAW264.7 cells that constitutively express Cas9 (RAW/Cas9). We then infected the library-transduced RAW/Cas9 cells [multi-plicity of infection (MOI) of 1] with MNV produced from a cDNA clone of MNV-S7-PP3 (MNV-S7) by our reverse-genetic system (14). The transduction caused no apparent CPE based on phase and fluorescent microscopy with Hoechst 33342 staining (Fig. 1*A*, *Left*). The subsequent infection by MNV killed most of the transduced cells (Fig. 1*A*, *Middle*). We reasoned that the few surviving cells had acquired resistance to MNV infection via the KO of an important gene that supports MNV infection.

To identify the gene(s) supporting MNV infection, we extracted the genomic DNA from the pooled population of cells that had escaped from the virus-induced CPE and amplified the ~180-bp fragments including the specific 20-bp region of the gRNA that had been integrated into the cell genome. By sequencing the PCR fragments with NGS, we identified the genes that were knocked out in the surviving cells. We performed the entire procedure from the library transduction to the NGS analysis twice independently. From these NGS results, 950 and 135 gRNA sequences with more than 10 reads were obtained in the first and second runs, respectively. The top six in descending order from the top of the read count are shown in Table S1. CD300lf was found in both independent experiments.

Mouse CD300lf (UniProtKB accession no. Q6SJQ7) is a member of the CD300 family, which modulates a broad and diverse array of immune-cell processes via paired activating and inhibitory receptors (17). CD300lf is an inhibitory receptor, and their paired activating
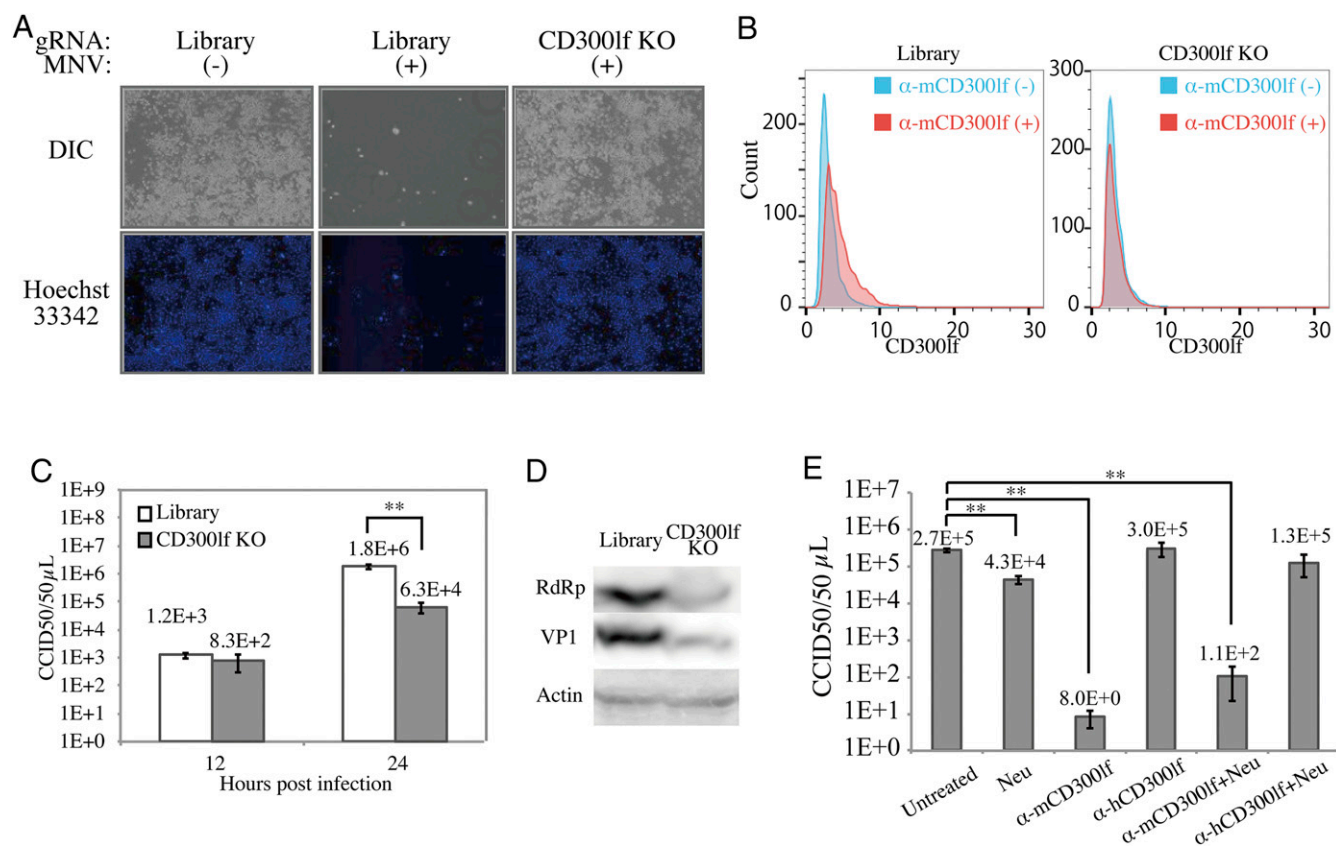

Fig. 1. CD300lf depletion decreases MNV production in RAW264.7 cells. (*A*) Microscopic images of RAW264.7 cells taken 48 h post inoculation with (+) or without (−) MNV. (*Upper*) Differential interference contrast (DIC) images. (*Lower*) Fluorescent images after Hoechst 33342 staining. The cells were transduced with a lentiviral gRNA library targeting sites throughout the murine genome (library) or with a lentiviral vector carrying gRNA specific to *CD300lf* (CD300lf KO). (*B*) Flow cytometric analysis of RAW/Cas9 cells transduced with lentiviral vector carrying the library (*Left*) or CD300lf KO (*Right*). Red and blue histograms indicate the cells that reacted or did not react with anti-CD300lf polyclonal antibody (α-mCD300lf), respectively. (*C*) MNV production in cells transfected with the library or CD300lf KO. Stably transfected cells were infected with MNV (MOI of 1) and incubated for 48 h. The titer is shown on a logarithmic scale. (*D*) Detection of VP1 and RdRp in MNV-infected RAW264.7 cells transfected with the library or CD300lf KO. Actin was used as a loading control. (*E*) MNV-S7 production in RAW264.7 cells. The cells were untreated or pretreated with neuraminidase (Neu; 50 mU/mL), antibodies to murine CD300lf (α-mCD300lf) or human CD300f (α-hCD300lf), or combinations thereof for 2 h at 37 °C. After pretreatment, the cells were infected with MNV (MOI of 0.05). The MNV titer in the cell supernatant at 48 hpi is shown on a logarithmic scale. Error bars represent the SD from three wells for each sample (**$P < 0.01$).

receptor is CD300ld. CD300lf is associated with the suppression of an allergic reaction with ceramide as a ligand (18). To determine if KO of CD300lf alone was linked to the loss of the MNV-induced CPE, we created CD300lf KO cells by introducing the gRNA targeting CD300lf into RAW/Cas9 cells (CD300lf KO cells). Challenged with MNV, no detectable CPE was observed in the CD300lf KO cells (Fig. 1A, Right). In contrast, cells transduced with several of the other gRNAs identified in the initial screens (Table S1) exhibited an MNV-induced CPE similar to that in the majority of the library-transduced cells.

To confirm that the functional *CD300lf* gene was lost in the CD300lf KO cells, we used FACS to detect CD300lf expression on the cell surface with an antibody obtained from a goat immunized with the mouse CD300lf extracellular domain (C16-G188). Exposure of the library-transduced RAW/Cas9 cells, representing the whole panel of cells containing the gRNA library, to the CD300lf antibody caused a slight shift in the FACS pattern of CD300lf-positive signal (Fig. 1B, red histogram) compared with the pattern produced by cells that were not exposed to the primary antibody (Fig. 1B, blue histogram), suggesting that CD300lf is expressed, albeit at low levels, on the surface of the cells (library gRNA; Fig. 1B, Left). The FACS pattern of the CD300lf KO cells was almost identical to that of the cells that were not exposed to the primary antibody (CD300lf KO; Fig. 1B, Right), suggesting that very little CD300lf was present on the CD300lf KO cell surface. After MNV exposure, the production of viral progeny was significantly reduced in the CD300lf KO cells (Fig. 1C). We harvested MNV-infected CD300lf KO cells at 48 hpi and performed Western blotting with antisera to the MNV-RNA–dependent RNA polymerase (α-RdRp) and the capsid viral protein 1 (α-VP1; Fig. 1D). The CD300lf KO cells showed significantly weaker VP1 and RdRp signals than those found in the library-transduced cells (Fig. 1D), suggesting that the CD300lf KO cells were defective in supporting MNV infection.

To determine whether CD300lf serves as an MNV receptor by directly binding to the virus, we attempted to block MNV infection with a set of polyclonal antibodies that differentially recognize the extracellular domains of mouse CD300lf (α-mCD300lf) and human CD300lf (α-hCD300lf). The binding of MNV to RAW264.7 cells was largely unaffected by the α-mCD300lf (Fig. S1A). Earlier reports noted that a glycan is involved in MNV binding (12, 13). Neuraminidase is reported to reduce MNV-1 binding to RAW264.7 cells. We therefore used neuraminidase treatment to remove the terminal sialic acid on RAW264.7 cells before MNV infection. The effect of neuraminidase was confirmed by fetuin deglycosylation (Fig. S1B); however, the neuraminidase treatment increased the MNV-S7 binding to RAW264.7 cells (Fig. S1A). We then measured the viral progeny production by quantitating the number of infectious MNV particles [cell-culture 50% infective dose ($CCID_{50}$)] in the culture supernatant of MNV-infected RAW264.7 cells after treatment with neuraminidase, α-mCD300lf, α-hCD300lf, or combinations thereof (Fig. 1E). The culture supernatant of the untreated, MNV-infected cells contained 2.7×10^5 $CCID_{50}$/50 µL infectious MNV particles at 48 hpi. In contrast, the culture supernatant of the cells treated with α-mCD300lf contained only 8.0×10^0 $CCID_{50}$/50 µL infectious MNV particles. The α-hCD300lf treatment produced no reduction in the yield of MNV infectious particles. The neuraminidase treatment reduced the yield of infectious MNV particles to 4.3×10^4 $CCID_{50}$/50 µL. The combination of neuraminidase and α-mCD300lf produced a yield of 1.1×10^2 $CCID_{50}$/50 µL infectious MNV particles. Similar results were obtained by using MNV-1 (Fig. S2). Those results suggest that the antibody against the murine CD300lf blocked MNV infection by interfering with the binding of the virus to CD300lf and the existence of other molecules that are involved in MNV binding to RAW264.7 cells, as α-mCD300lf did not reduce MNV binding on the cell surface.

CD300lf Expression Changes the Susceptibility of Cells to MNV. We obtained cDNA of murine CD300lf (UniProt KB accession no. LC131461) from mRNA extracted from RAW264.7 cells. We cloned the *CD300lf* cDNA into a lentiviral vector and used the vector to constitutively express murine CD300lf in HEK293T cells, which are not permissive to MNV infection. After transduction and puromycin selection, we confirmed the expression of CD300lf in the transduced HEK293T cells (CD300lf cells) by FACS analysis with α-mCD300lf as the primary antibody. Comparison with mock-transduced HEK293T cells ("mock cells") clearly showed that CD300lf was expressed on the surface of the CD300lf cells (Fig. 2A). We then determined if purified MNV could bind to the CD300lf cells. FACS analysis revealed a fluorescein-positive population of CD300lf cells after exposure to MNV that was distinct from the population of mock cells, suggesting that CD300lf mediates MNV binding to the cells (Fig. 2B). After MNV infection, Western blotting revealed VP1 and RdRp in the CD300lf cells but not in the mock cells (Fig. 2C). Upon MNV infection, the parental HEK293T cells produced little infectious MNV progeny (4.4×10^0 $CCID_{50}$/50 µL; Fig. 2D), whereas the CD300lf cells produced abundant MNV progeny (1.22×10^6 $CCID_{50}$/50 µL). Those results indicate that the expression of CD300lf in HEK293T cells was sufficient to render those nonpermissive cells susceptible to MNV infection.

To determine if CD300lf could render cells from different hosts susceptible to MNV infection, we transduced CD300lf into CRFK cells from cat, CHO cells from Chinese hamster, COS7 cells from African green monkey, and NIH 3T3 cells from mouse and established cell lines that stably expressed CD300lf. We confirmed the CD300lf expression by FACS analysis of each cell line based on a positive shift of the signal peaks indicating reaction with CD300lf-specific antibody (Fig. 2E). After infection with MNV, we detected the expression of RdRp and VP1 by Western blotting in the CD300lf-expressing cells but not in the control parental cells (Fig. 2F). The CD300lf-expressing cells produced approximately 10^3–10^5 $CCID_{50}$/50 µL MNV progeny, whereas the control cells produced 1–10^2 $CCID_{50}$/50 µL MNV progeny, which was lower than the inoculum titer, indicating that viral growth in the cells was dependent on the presence of CD300lf (Fig. 2G). Those results further documented that CD300lf dictates the permissiveness of cells to MNV.

Finally, we used a genetically defined MNV-S7 clone produced by our reverse-genetic system to infect CD300lf cells. We serially passaged the viral clone three times and then sequenced its genome by using NGS. After passage in the CD300lf cells, the viral genome displayed no nucleotide changes compared with the original pMNV-S7 sequence (GenBank accession no. AB435515). Similarly, we serially passaged another strain of MNV (MNV-1) in CD300lf cells three times and analyzed its genome by NGS. The sequence of the passaged genome completely matched that of the original cDNA (GenBank accession no. NC_008311).

Examination of the Minimum Extracellular Domain of CD300lf Required to Bind MNV. To further define the role of CD300lf as an MNV receptor, we constructed the full-length CD300lf (henceforth "FL") and four deletion mutants (Δ130–170, ΔCterm, Δ18–51, and Δcpd; Figs. S3 and S4) and tested them to determine whether the expressed proteins could function as the receptor for MNV infection in HEK293T cells. We transfected each construct into HEK293T cells and then infected the cells with MNV 24 h later. All constructs except for ΔCterm were expressed on the cell surface (Fig. 3A, Left). MNV was able to bind to the cells expressing FL, Δ130–170, or Δcpd but not to those expressing ΔCterm or Δ18–51 (Fig. 3A, Right). We evaluated the ability of the cells to support MNV infection based on the expression of RdRp and VP1 at 48 hpi as shown by Western blotting. The cells expressing FL, Δ130–170, or Δcpd contained both viral proteins, whereas those expressing ΔCterm or Δ18–51 contained neither viral protein (Fig. 3B). We detected MNV progeny in the supernatants
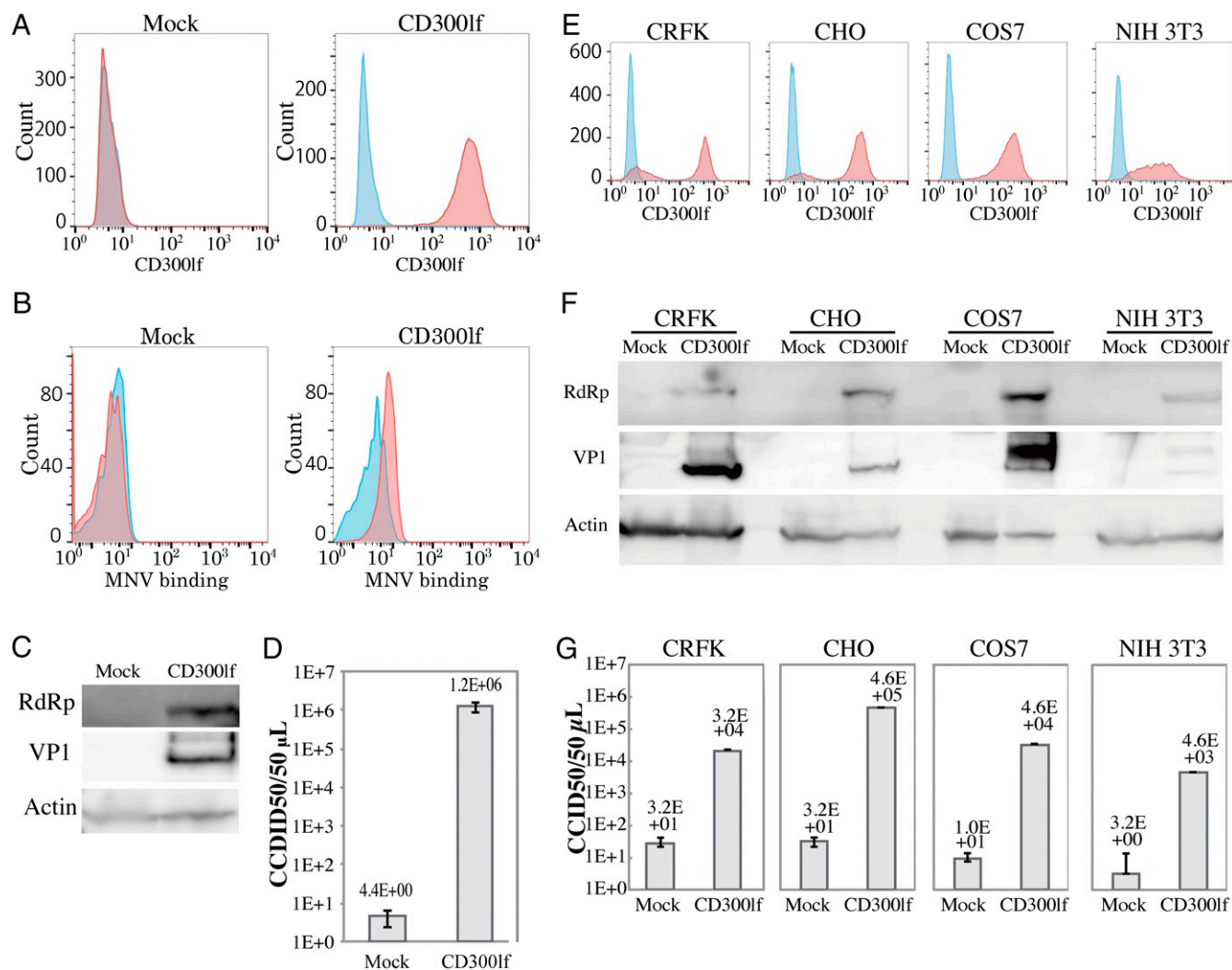
Fig. 2. HEK293T cells expressing CD300lf are susceptible to MNV infection. Flow cytometry was performed with HEK293T cells mock transfected or transduced with a CD300lf expression vector. (*A*) Immunofluorescence staining with [α-mCD300lf(+); red histogram] or without [α-mCD300lf(−); blue histogram] anti-CD300lf antibody. (*B*) The cells were incubated in the absence [MNV(−); blue histogram] or presence [MNV(+); red histogram] of MNV. The cells bound to the MNV were immunostained by using an anti-MNV VP1 antibody. The *x*-axes represent the extent of CD300lf expression (*A*) and MNV binding (*B*). (*C*) Detection of VP1 and RdRp after MNV infection in the cells described earlier. Actin was evaluated as the loading control. (*D*) MNV production in HEK293T/CD300lf cells. The MNV titer in the supernatant of infected cells (MOI of 1) is shown. (*E*) Mammalian cell lines CRFK, CHO, COS7, and NIH 3T3 transduced with CD300lf became susceptible to MNV. Flow cytometry of the four cell lines was performed to measure CD300lf expression. Red and blue histograms indicate CD300lf-transduced and mock cells, respectively. (*F*) MNV production in CD300lf-expressing cell lines was examined by the detection of RdRp and VP1 expression by Western blotting. (*G*) $CCID_{50}/50$ μL of viral progeny produced from each CD300lf-expressing cell line at 48 hpi. Error bars represent the SD from three wells for each sample.

from the cells expressing FL, Δ130–170, or Δcpd (Fig. 3*C*). Those data indicate that the CD300lf region deleted in Δ130–170 and the cytoplasmic domain are dispensable for MNV infection, whereas the expression of the CD300lf on cell surface via their transmembrane domain is essential for MNV receptor. Furthermore, the MNV-binding site of CD300lf is located among the 34 amino acids at the N terminus of the protein, and that region has an important function as an MNV receptor.

The N-Terminal Region of CD300lf Is Important for MNV Infection, and Its Paired Receptor CD300ld also Functions as an MNV Receptor. To evaluate the possible docking conformation of an MNV-S7 and CD300lf complex, we performed a protein–protein docking simulation by using the Dock application in the Molecular Operating Environment (MOE) with a CD300lf structure file from Research Collaboratory for Structural Bioinformatics-Protein Data Bank (RCSB-PDB; Fig. S5) and a cryo-EM image of the MNV-S7 P domain (Fig. S6). The obtained docking model suggests that CD300lf could dock to the

β-hairpin in the P1 subdomain located at the interface of the P2 subdomain dimer (Fig. 4*A*, *Left*). CD300lf was predicted to form hydrogen bonds and ionic interactions with the β-hairpin and loop in the MNV-S7 P domain. From the modeling, we also predicted that the N-terminal acetyl, P26, R42, and R88 of CD300lf might bind the K345, D440, D443, and D403 residues, respectively, of the MNV VP1 protein (Fig. 4*A*, *Right*). Those residues of VP1 are conserved in the MNV-S7, MNV-1, and CR3 strains. The predicted binding residues of VP1 are located in the P2 and P1 domains. Based on those predictions, we mutated each residue of CD300lf to alanine and expressed the mutated proteins in HEK293T cells (Fig. 4*B*, *Left*). Contrary to our expectations, we found that MNV was able to bind to HEK293T cells expressing each mutated protein (Fig. 4*B*, *Right*). The tertiary structure of the CD300lf extracellular domain (PDB ID code 1ZOX; Fig. S5) showed that the Δ18–51 region includes three β-sheets (VT, EVSGQ, and LTVQCRY) and also helices (SGW). In addition, R42 was located in the third β-sheet, and
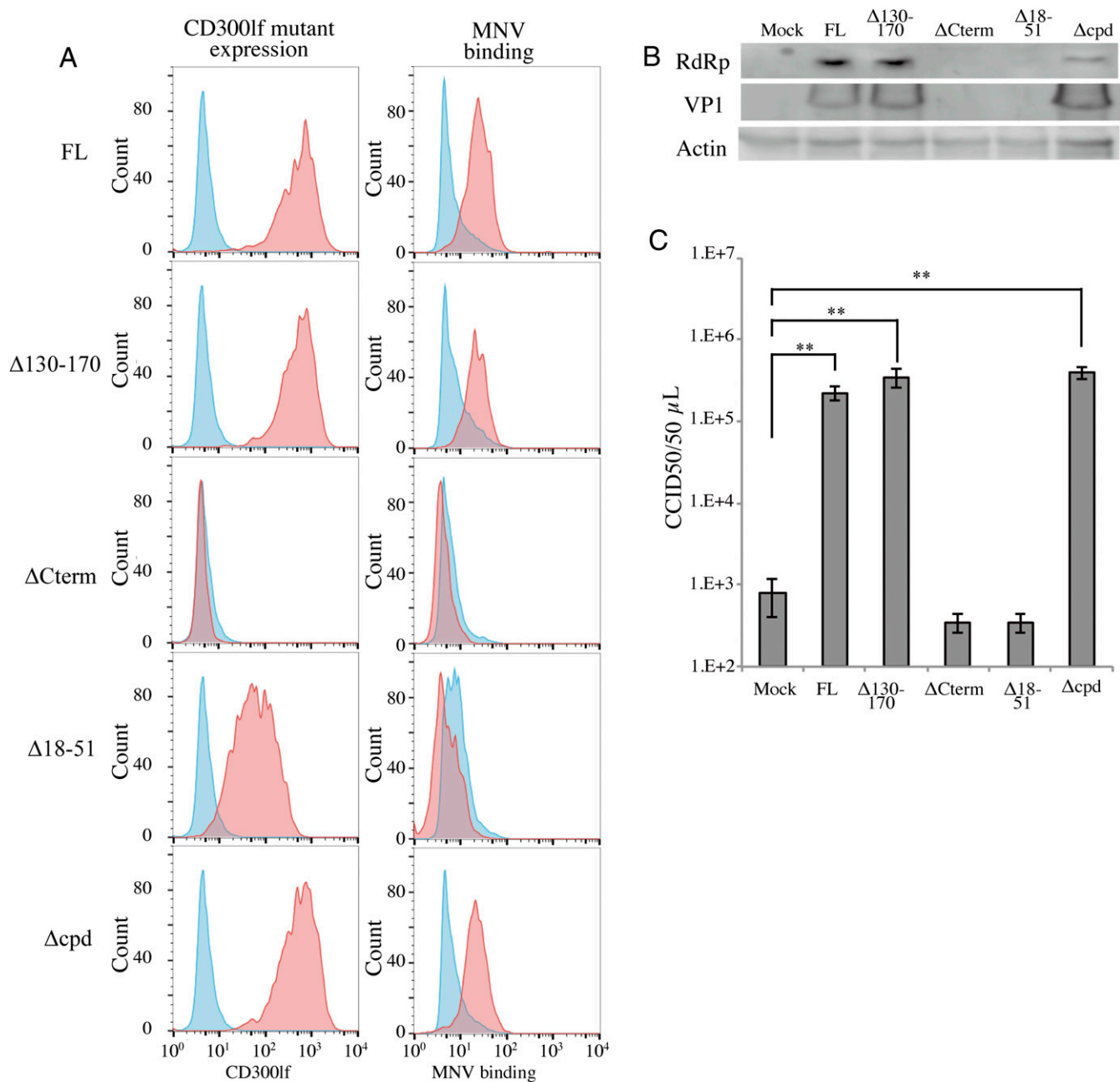
Fig. 3. The N-terminal region of CD300lf is important for MNV infection in HEK293T cells. (*A*) HEK293T cells cotransduced with GFP and FL, Δ130–170, ΔCterm, Δ18–51, or Δcpd were examined for CD300lf expression (*Left*) and MNV binding (*Right*). (*Left*) Overlay histograms of the GFP-gated cells expressing [αCD300lf(+); red histogram] or not expressing [αCD300lf(−); blue histogram] CD300lf. (*Right*) Overlay histograms of the MNV binding [GFP(+), red histogram; GFP(−), blue histogram]. (*B*) HEK293T cells expressing the CD300lf variants or no construct (mock) were infected with MNV. Viral protein expression was analyzed by Western blotting. RdRp and VP1 in CD300lf cells expressing FL, Δ130–170, ΔCterm, Δ18–51, or Δcpd were probed with anti-RdRp and anti-VP1 antibodies, respectively. Actin was used as a loading control. (*C*) MNV titer in the supernatant of HEK293T cells expressing FL, Δ130–170, ΔCterm, Δ18–51, or Δcpd at 48 hpi. Error bars represent the SD from three wells for each sample (**$P < 0.01$).

the CD300lf-specific gRNA targeted a part of the third β-sheet and the helices. Therefore, we produced another mutant CD300lf construct with seven amino acids deleted (Δ39–45) where it is targeted by the gRNA and transfected that construct into HEK293T cells. Although we confirmed the expression of the Δ39–45 protein on the cell surface by FACS, MNV could not bind to the cell surface, and viral progeny were not produced (Fig. 4 *C* and *D*). Although it is still unclear whether MNV directly binds the region of amino acid residues 39–45, those data suggest that this region of CD300lf plays an important role in MNV binding.

The amino acid sequence of the N-terminal region of the CD300lf extracellular domain is highly homologous to that of the paired receptor CD300ld (Fig. S7). The difference between CD300lf and CD300ld lies within the cytoplasmic domain, which was shown to be dispensable to CD300lf function as an MNV receptor. To determine if CD300ld functions as an MNV receptor, we cloned CD300ld (UniProt KB accession no. LC132714) from the mRNA of RAW264.7 cells and transfected it into HEK293T cells. We confirmed CD300ld expression on the cell surface by FACS. MNV was able to bind to the CD300ld-expressing cells.
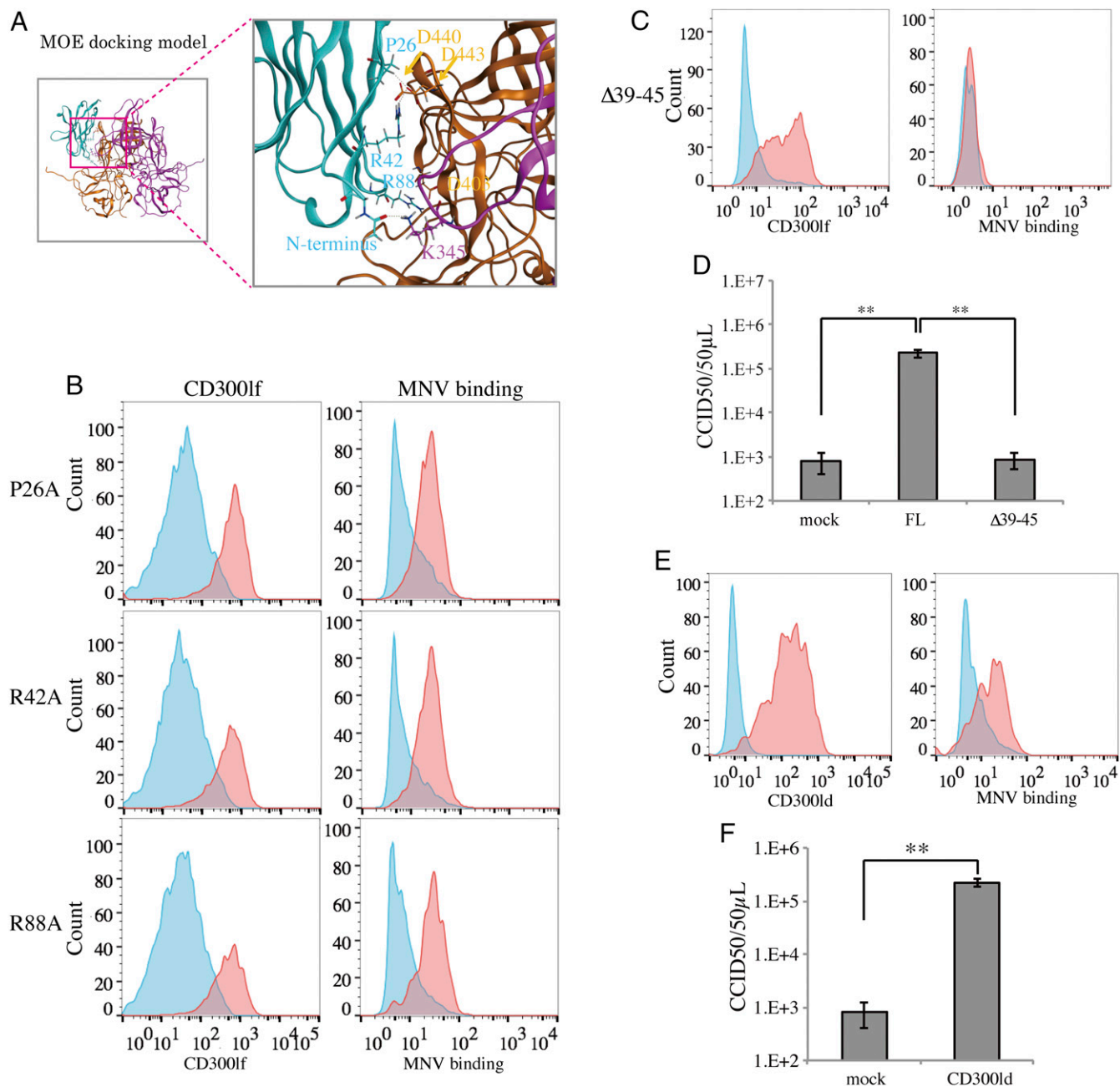
Haga et al.

Fig. 4. Docking model of the MNV-S7 capsid P-domain dimer and the CD300lf extracellular domain. (*A*) The docking simulation was performed by using the Dock application in MOE software. The overall structure of the docking model (*Left*) and an enlarged view of the interface of MNV-S7 and CD300lf (*Right*) are shown. The orange and magenta ribbons and the cyan ribbon are MNV-S7 and CD300lf, respectively. The colored sticks show the residues that form the hydrogen bonds (gold dotted line) or ionic interactions between MNV-S7 and CD300lf. (*B*, *C*, and *E*) HEK293T cells cotransduced with GFP and CD300lf mutants were analyzed for CD300lf expression (*Left*) and MNV binding (*Right*). (*Left*) Overlaid histograms of the GFP-gated cells expressing [αCD300lf(+); red histogram] and not expressing [αCD300lf(−); blue histogram] CD300lf. (*Right*) Overlaid histograms of the MNV binding [GFP(+), red histogram; GFP(−), blue histogram]. (*D* and *F*) MNV titer in the supernatant of HEK293T cells mock-transduced or transduced with the constructs expressing Δ39–45 or CD300ld at 48 hpi. Error bars represent the SD from three wells for each sample (**$P < 0.01$).

Upon infection with MNV, those cells produced MNV progeny at the same level as CD300lf-expressing HEK293T cells (Fig. 4 *E* and *F*). Those data show that CD300ld functions as an MNV receptor.

Discussion

In this paper, we report CD300lf and CD300ld as functional receptors for MNV infection. By using a genome-wide KO screening with a lentiviral vector carrying a gRNA library, we found that the depletion of CD300lf caused resistance to MNV in RAW264.7

cells, which are known to be permissive to MNV infection. In addition, a polyclonal antibody specific to murine CD300lf blocked MNV infection of RAW264.7 cells, but an antibody specific to the human homolog had no effect. When we introduced CD300lf into cells that were not originally permissive to MNV infection, CD300lf expression made the cells permissive to MNV infection. By using a set of deletion mutants, we determined that the N-terminal region of CD300lf, spanning amino acids 39–45, is important (necessary and sufficient) for the binding and entry of MNV into nonpermissive

cells. The ectopic expression of murine CD300ld, which has an extracellular domain highly similar to that of CD300lf, in HEK293T cells rendered the cells permissive to MNV infection. Therefore, CD300lf and CD300ld are cellular receptors for MNV, and the extracellular domains of those proteins confer species specificity to the viral infection.

We used a CRISPR/Cas9-based genome-wide gene-editing system to identify the cellular receptors for MNV in RAW264.7 cells. Only one of the six gRNAs that target *CD300lf* in the CRISPR/Cas9 library used in our study rendered the cells resistant to MNV infection (Fig. 1*A*, *Right*). The deletion caused by that gRNA (Δ39–45) abolished the MNV-receptor function of CD300lf upon expression in HEK293T cells, as shown by a lack of MNV binding and an inability to support MNV infection (Fig. 4 *C* and *D*). Those data suggest that the region targeted by the *CD300lf* gRNA is important for receptor function through interaction with MNV. The functional KO of CD300lf in RAW264.7 cells did not completely prevent the production of MNV progeny (Fig. 1*C*). That result led to the discovery of CD300ld as another receptor for MNV (Fig. 4 *E* and *F*). The N-terminal region of CD300ld is highly homologous to that of CD300lf (Fig. S7). In the initial genome-wide screening, CD300ld did not emerge as a candidate gene to prevent MNV infection. Close inspection of the four *CD300ld*-specific gRNAs included in the library revealed that none of them targeted the N-terminal region of CD300ld. Therefore, we speculated that the gene editing by the *CD300ld*-specific gRNAs did not create a functional KO of CD300ld. Because of the homology between CD300lf and CD300ld, the commercially available antibody that reacted with the N-terminal region of CD300lf (AF2788; R&D Systems) also reacted with CD300ld expressed on 293T/CD300ld cells (Fig. 4*E*). The blocking of MNV infection mediated by the anti-CD300lf antibody (Fig. 1 *D* and *E*) appeared to be more effective than that mediated by the *CD300lf*-specific gRNA (Fig. 1*C*), suggesting that the antibody blocked both CD300ld and CD300lf, which are homologous in their respective MNV-binding regions.

The extracellular domains of CD300lf and CD300ld are highly homologous; the 112 aa distal to the signal-peptide sequence encompass the N-terminal region and showed 85.7% homology between the two molecules (Fig. S7). The two motifs in the N-terminal region of CD300lf, from P22 to C55 and from E68 to K113, were 94.1% and 93.3% identical to those in CD300ld, respectively. Our results showed that the former motif harbored residues important for MNV binding. Two sets of deletions in CD300lf, Δ18–51 and Δ39–45, abrogated the ability of CD300lf to facilitate MNV infection in HEK293T cells, indicating that residues 39–45 of CD300lf (VQCRYTS) are necessary for the interaction with MNV (Figs. 3 and 4 *C* and *D*). It is still unclear, however, whether MNV directly binds to the 39–45 region or the deletion of that region led to a structural change that resulted in the lack of MNV binding. Although we did not demonstrate it experimentally, we postulate that the corresponding residues in the N-terminal region of CD300ld (VQCRYSS) are similarly important for MNV binding. In the structural model of CD300lf, the residues VQCRYTS resided within the third β-sheet and were well exposed. The docking model of the CD300lf–VP1 complex predicted that one of those seven residues interacts with VP1 (Fig. 4*A*). Although our search for the interactive residues based on the model was unsuccessful, it is essential to define the key interactions for the binding of VP1 to CD300lf and CD300ld to understand the molecular nature of MNV entry into cells, which will be the focus of our next study.

Unlike the residues in the N-terminal region, the residues in the C-terminal region, encompassing the transmembrane and cytoplasmic domains, differ significantly between CD300lf and CD300ld (Fig. S7). CD300lf has a tyrosine motif for endocytosis located in the cytoplasmic domain, but that motif is dispensable for MNV infection (Fig. 3). CD300ld binds to FcRγ and DAP12 through the immunoreceptor tyrosine-based activating motif in the transmembrane domain, which causes signal transduction (19). One

would expect that, upon binding to the virus, the receptor molecule would mediate a series of cellular events that facilitate viral entry into the cell, although the current knowledge of CD300lf and CD300ld provides few clues about the specific role of those molecules in the viral entry process. Unknown cofactors might interact with CD300lf and CD300ld in the homologous N-terminal regions to help with MNV internalization.

In leukocytes, the CD300 family proteins on the membranes of myeloid cells are regulatory molecules involved in the stimulation or suppression of cell functions (17). CD300lf and CD300ld work together as paired receptors, probably recognizing the same ligand as they work in opposite ways to maintain cellular homeostasis (17). The expression of CD300lf and CD300ld is restricted to granulocytes, bone-marrow mast cells, and dendritic cells. Macrophages and dendritic cells are targets of MNV (20), making CD300lf and CD300ld biologically relevant for MNV infection.

The expression levels of CD300ld and CD300lf in RAW264.7 cells are considered low and absent, respectively, based on transcriptional analyses (21). The ectopic CD300lf expression on the HEK293T cell surface appeared to be higher than that on the RAW264.7 cell surface based on the fluorescent signals of CD300lf expression (Figs. 1*B* and 2*A*). The extent of CD300lf expression did not impact the production of viral progeny in HEK293T/CD300lf cells (Figs. 1*C* and 2*D*). Although our data show that CD300lf and CD300ld are protein receptors that confer susceptibility to MNV, other factors on the cell surface might enhance MNV infection in RAW264.7 cells. The polyclonal antibody to mCD300lf strongly inhibited the production of MNV progeny (Fig. 1*E*) but did not reduce MNV binding (Fig. S1*A*), indicating that other factors, such as sialic acid and other sugar moieties, are involved in MNV binding. Recently, cell-surface proteins of macrophages and dendritic cells were shown to be involved in MNV-1 binding (22). Those proteins might function as an initial attachment site, creating opportunities for MNV to subsequently bind to CD300lf or CD300ld. Furthermore, two MNV strains, MNV-1 and CR3, demonstrate different tissue tropisms, and surface glycan molecules were reported to play a role as determinants of the tropism (12, 13). Our data revealed that not only MNV-S7, but also MNV-1, infects cells in a CD300lf-dependent manner. Further investigation is required to reveal whether the tissue tropism is defined by virus-specific characteristics or by the existence of other molecules on the cell surface that help MNV to bind to CD300lf or CD3001d.

Norovirus infections exhibit strict host tropism. HuNoV infection leading to efficient and reproducible viral growth is restricted to humans. The infection of chimpanzees by HuNoV via intravenous injection resulted in limited viral growth (23). Suboptimal HuNoV growth in the intestinal tract, detected based on the presence of viral antigen, was reported in gnotobiotic pigs (22). A low level of subclinical HuNoV growth was reported in BALB/c-mice deficient in Rag and common γ-chain (24). The replication of the norovirus RNA and the production of viral progeny are not restricted, however, to the cells of the natural host: HuNoV genomic RNA introduced into mammalian cells of human or simian origin can replicate and initiate the production of viral particles that package genomic RNA, although the virus does not spread (14). Similarly, MNV virions that are infectious to RAW264.7 cells can be produced in human cells (e.g., HEK293T, Huh7, Caco2, and Intestine 407 cells) as well as in simian cells by introducing plasmid constructs that express the MNV genomic RNA (14). The difference between the infection and transduction of the viral genomic nucleotides that prime viral replication lies in the interaction of the virus with cell-surface molecules, namely the cell-entry steps, which appear to shape the host tropism of the noroviruses. The fact that nonmurine mammalian cells expressing CD300lf or CD300ld become permissive to MNV infection (Figs. 2 and 4 *E* and *F*) indicates that CD300lf and CD300ld are sufficient alone to make cells susceptible to MNV. The results provide clear evidence that

the interaction of the virus with the cellular receptor dictates noroviral host tropism. The present findings provide a foundation to open up new research to fully understand the mechanisms of norovirus entry into cells. This could be especially important in enhancing the study of HuNoVs, for which cell-culture systems that efficiently support the full viral infection cycle are not available.

Materials and Methods

Cell Culture and MNV Strain. The cultured cell lines HEK293T [American Type Culture Collection (ATCC)], CRFK (ATCC), CHO, and NIH 3T3 (gift from Yuichi Someya, National Institute of Infectious Diseases) were maintained in DMEM supplemented with 10% (vol/vol) FBS. The RAW264.7 cell line (ATCC) was maintained in DMEM supplemented with 10% (vol/vol) FBS and 2.5 mM HCl. The MNV-S7 virus was produced by using a plasmid-based reverse-genetic system in HEK293T cells and then propagated further in RAW264.7 cells. The MNV-1 was a gift from Ian Goodfellow, University of Cambridge, Cambridge, UK and was propagated in RAW264.7 cells. Polyclonal goat IgG specific for the extracellular domain of mouse CD300lf (AF2788; R&D Systems), polyclonal goat IgG specific for the extracellular domain of human CD3001f (AF2774; R&D Systems), and neuraminidase (N7885; Sigma) were used in the inhibition assays of MNV production in RAW264.7 cells. Those treatments were incubated in DMEM without FBS.

Library Screening with NGS. The genomic DNA of RAW cells that survived the MNV-induced CPE was extracted by Nucleospin tissue XS (Takara Bio). The integrated gRNA regions were amplified by PCR with forward primer 5-GACTAT-CATATGCTTACCGTAAC-3 and reverse primer 5-AAAAAGCACCGACTCGGTGCCAC-3. The PCR products, ~180 bp in size, were sequenced by NGS. The basic methods used in the NEBNext Ultra RNA Library Prep Kit for Illumina (New England Biolabs) were described previously (25). The PCR products were treated according to the "end repairing and dA-tailing" section of the manufacturer's instructions. Nucleotide sequencing was performed with a MiSeq sequencer (Illumina) using a MiSeq Reagent Kit v2 (Illumina) to generate 151-bp paired-end reads. The FASTQ files from MiSeq were analyzed by using CLC Genomic Workbench 8.0 (Qiagen-CLC Bio).

Flow Cytometric Analysis. The expression of CD300lf and CD300ld was analyzed by FACS analysis. The cells were detached from plates by using enzyme-free dissociation buffer (Gibco). Goat anti-CD300lf polyclonal antibodies (AF2788; R&D Systems), which cross-react with CD300ld, were reacted with the cells for 30 min. Then, the cells were washed and incubated with phy-coerythrin-conjugated donkey anti-goat IgG (sc-3743; Santa Cruz Biotechnology) for 30 min. Afterward, the cells were washed and subjected to analysis. All staining and washing steps were carried out in ice-cold phosphate-buffered saline without magnesium and calcium salts [PBS(–)] solution supplemented with 0.5% FCS, 5 mM EDTA, and 0.1% NaN₃. The cells were analyzed using a FACSCalibur flow cytometry system (BD) and analyzed by using FlowJo software.

Evaluation of MNV Binding. MNV binding to cells was determined by FACS analysis. Briefly, 2×10^5 cells were incubated with 10 μg purified, infectious MNV for 30 min at 4 °C. After washing, the cells were incubated with anti-MNV VP1 rabbit polyclonal antibody for 30 min. Then, the cells were washed and incubated with PE-conjugated donkey anti-rabbit IgG (711-116-152; Jackson ImmunoResearch) for 30 min. Afterward, the cells were washed again and analyzed. For experiments with transiently expressing cells, GFP-encoded plasmids, used as a transfection marker, were cotransfected into HEK293T cells. The GFP-positive cells were selectively sorted by FACS based on the expression of CD300lf or the CD300lf mutants.

MNV Titration Using CCID₅₀. Tenfold serially diluted culture fluid containing MNV was prepared in 96-well plates, and 2.5×10^4 RAW cells were added into each well. The CCID₅₀ of the MNV was calculated from triplicate assays at 48 hpi.

In Silico Docking Model of MNV-S7 and CD300lf. The docking model of the MNV-S7 capsid P-domain dimer and the CD300lf extracellular domain was constructed by using the Dock application in the MOE 2015.10 (Chemical Computing Group). The docking simulation used the cryo-EM structure of the MNV-S7 capsid P-domain dimer described in *SI Materials and Methods* and Fig. S6 and the crystal structure of the mouse CD300lf extracellular domain at a resolution of 2.1 Å (PDB ID code 1ZOX). We obtained 100 poses by using the docking simulation and selected the model with the best score and physically acceptable pose.

Statistics. All statistical analyses were performed on GraphPad Prism version 6.0 for Macintosh (GraphPad Software). Groups were compared by using the Student's t test with statistical significance determined using the Holm–Sidák method. P values < 0.05 were considered statistically significant.

1. Kapikian AZ, et al. (1972) Visualization by immune electron microscopy of a 27-nm particle associated with acute infectious nonbacterial gastroenteritis. *J Virol* 10(5):1075–1081.
2. Jones MK, et al. (2014) Enteric bacteria promote human and mouse norovirus infection of B cells. *Science* 346(6210):755–759.
3. Ruvoën-Clouet N, Ganière JP, André-Fontaine G, Blanchard D, Le Pendu J (2000) Binding of rabbit hemorrhagic disease virus to antigens of the ABH histo-blood group family. *J Virol* 74(24):11950–11954.
4. Hutson AM, Atmar RL, Graham DY, Estes MK (2002) Norwalk virus infection and disease is associated with ABO histo-blood group type. *J Infect Dis* 185(9):1335–1337.
5. Kambhampati A, Payne DC, Costantini V, Lopman BA (2016) Host genetic susceptibility to enteric viruses: A systematic review and metaanalysis. *Clin Infect Dis* 62(1):11–18.
6. Marionneau S, et al. (2002) Norwalk virus binds to histo-blood group antigens present on gastroduodenal epithelial cells of secretor individuals. *Gastroenterology* 122(7):1967–1977.
7. Cheetham S, et al. (2007) Binding patterns of human norovirus-like particles to buccal and intestinal tissues of gnotobiotic pigs in relation to A/H histo-blood group antigen expression. *J Virol* 81(7):3535–3544.
8. Murakami K, et al. (2013) Norovirus binding to intestinal epithelial cells is independent of histo-blood group antigens. *PLoS One* 8(6):e66534.
9. Huang P, et al. (2005) Norovirus and histo-blood group antigens: Demonstration of a wide spectrum of strain specificities and classification of two major binding groups among multiple binding patterns. *J Virol* 79(11):6714–6722.
10. Guix S, et al. (2007) Norwalk virus RNA is infectious in mammalian cells. *J Virol* 81(22):12238–12248.
11. Karst SM, Wobus CE, Lay M, Davidson J, Virgin HW, 4th (2003) STAT1-dependent innate immunity to a Norwalk-like virus. *Science* 299(5612):1575–1578.
12. Taube S, et al. (2009) Ganglioside-linked terminal sialic acid moieties on murine macrophages function as attachment receptors for murine noroviruses. *J Virol* 83(9):4092–4101.
13. Taube S, et al. (2012) Murine noroviruses bind glycolipid and glycoprotein attachment receptors in a strain-dependent manner. *J Virol* 86(10):5584–5593.
14. Katayama K, et al. (2014) Plasmid-based human norovirus reverse genetics system produces reporter-tagged progeny virus containing infectious genomic RNA. *Proc Natl Acad Sci USA* 111(38):E4043–E4052.
15. Kitagawa Y, et al. (2010) Indirect ELISA and indirect immunofluorescent antibody assay for detecting the antibody against murine norovirus S7 in mice. *Exp Anim* 59(1):47–55.
16. Koike-Yusa H, Li Y, Tan EP, Velasco-Herrera MdelC, Yusa K (2014) Genome-wide recessive genetic screening in mammalian cells with a lentiviral CRISPR-guide RNA library. *Nat Biotechnol* 32(3):267–273.
17. Borrego F (2013) The CD300 molecules: An emerging family of regulators of the immune system. *Blood* 121(11):1951–1960.
18. Izawa K, et al. (2014) Sphingomyelin and ceramide are physiological ligands for human LMIR3/CD300f, inhibiting FcepsilonRI-mediated mast cell activation. *J Allergy Clin Immunol* 133(1):270–273.
19. Comas-Casellas E, et al. (2012) Cloning and characterization of CD300d, a novel member of the human CD300 family of immune receptors. *J Biol Chem* 287(13):9682–9693.
20. Wobus CE, et al. (2004) Replication of Norovirus in cell culture reveals a tropism for dendritic cells and macrophages. *PLoS Biol* 2(12):e432.
21. Clark GJ, Ju X, Tate C, Hart DN (2009) The CD300 family of molecules are evolutionarily significant regulators of leukocyte functions. *Trends Immunol* 30(5):209–217.
22. Cunha JB, Wobus CE (2016) Select membrane proteins modulate MNV-1 infection of macrophages and dendritic cells in a cell type-specific manner.. *Virus Res* 222:64–70.
23. Bok K, et al. (2011) Chimpanzees as an animal model for human norovirus infection and vaccine development. *Proc Natl Acad Sci USA* 108(1):325–330.
24. Taube S, et al. (2013) A mouse model for human norovirus. *MBio* 4(4):e00450-13.
25. Dennis FE, et al. (2014) Identification of novel Ghanaian G8P[6] human-bovine reassortant rotavirus strain by next generation sequencing. *PLoS One* 9(6):e100699.
26. Haga K, et al. (2007) Efficient immortalization of primary human cells by p16INK4a-specific short hairpin RNA or Bmi-1, combined with introduction of hTERT. *Cancer Sci* 98(2):147–154.
27. Tang G, et al. (2007) EMAN2: An extensible image processing suite for electron microscopy. *J Struct Biol* 157(1):38–46.
28. Scheres SH (2012) RELION: Implementation of a Bayesian approach to cryo-EM structure determination. *J Struct Biol* 180(3):519–530.
29. Rosenthal PB, Henderson R (2003) Optimal determination of particle orientation, absolute hand, and contrast loss in single-particle electron cryomicroscopy. *J Mol Biol* 333(4):721–745.
30. Pettersen EF, et al. (2004) UCSF Chimera–a visualization system for exploratory research and analysis. *J Comput Chem* 25(13):1605–1612.